Cell Death &
Differentiation

ARTICLE

IL-24 deficiency protects mice against bleomycin-induced pulmonary fibrosis by repressing IL-4-induced M2 program in macrophages

Li-Zong Rao[1,2] · Yi Wang[2] · Lei Zhang[2] · Guorao Wu[2] · Lu Zhang[2] · Fa-Xi Wang[2] · Long-Min Chen[2] · Fei Sun[2] · Song Jia[2] · Shu Zhang[2] · Qilin Yu[2] · Jiang-Hong Wei[3] · Hui-Ren Lei[3] · Ting Yuan[2,3] · Jinxiu Li[4] · Xingxu Huang [ID][5] · Bin Cheng[6] · Jianping Zhao[2] · Yongjian Xu[2] · Bi-Wen Mo[3] · Cong-Yi Wang [ID][2] · Huilan Zhang[2]

Abstract

Idiopathic pulmonary fibrosis (IPF) is the most common type of idiopathic interstitial pneumonia and has one of the poorest prognosis. However, the molecular mechanisms underlying IPF progression remain largely unknown. In this study, we determined that IL-24, an IL-20 subfamily cytokine member, was increased both in the serum of IPF patients and the bronchoalveolar lavage fluid (BALF) of mice following bleomycin (BLM)-induced pulmonary fibrosis. As a result, *IL-24* deficiency protected mice from BLM-induced lung injury and fibrosis. Specifically, loss of *IL-24* significantly attenuated transforming growth factor β1 (TGF-β1) production and reduced M2 macrophage infiltration in the lung of BLM-induced mice. Mechanistically, IL-24 alone did not show a perceptible impact on the induction of M2 macrophages, but it synergized with IL-4 to promote M2 program in macrophages. IL-24 suppressed IL-4-induced expression of suppressor of cytokine signaling 1 (SOCS1) and SOCS3, through which it enhanced signal transducer and activator of transcription 6/peroxisome proliferator-activated receptor gamma (STAT6/PPARγ) signaling, thereby promoting IL-4-induced production of M2 macrophages. Collectively, our data support that IL-24 synergizes with IL-4 to promote macrophage M2 program contributing to the development of pulmonary fibrosis.

These authors contributed equally: Li-Zong Rao, Yi Wang

Edited by M. Bianchi

✉ Bi-Wen Mo
mobiwen2002@sohu.com

✉ Cong-Yi Wang
wangcy@tjh.tjmu.edu.cn

✉ Huilan Zhang
huilan_76@163.com

1 Department of Respiratory and Critical Care Medicine, Key Laboratory of National Clinical Research Center for Respiratory Disease, Xiangya Hospital, Central South University, 87 Xiangya Road, Changsha, 410000 Hunan, China

2 The Center for Biomedical Research, Department of Respiratory and Critical Care Medicine, NHC Key Laboratory of Pulmonary Diseases, Key Cite of National Clinical Research Center for

Respiratory Disease, Wuhan Clinical Medical Research Center for Chronic Airway Diseases, Tongji Hospital, Tongji Medical College, Huazhong University of Sciences and Technology, 1095 Jiefang Ave, Wuhan, 430030, China

3 Department of Respiratory and Critical Care Medicine, The Affiliated Hospital of Guilin Medical University, 15 Lequn Road, Guilin, 541000 Guangxi, China

4 ICU Division, Xiangya Second Hospital, Central South University, Changsha, 410011 Hunan, China

5 School of Life Science and Technology, Shanghai Tech University, Shanghai, 201210, China

6 Department of Gastroenterology and Hepatology, Tongji Hospital, Tongji Medical College, Huazhong University of Science and Technology, Wuhan, 430030, China

Introduction

Idiopathic pulmonary fibrosis (IPF) is a severe health problem worldwide. Although the incidence of IPF is only 2.8–18 cases/100,000 per year [1, 2], the average survival time after diagnosis, however, is as low as 2–4 years [3]. Previous studies have demonstrated that the

pathogenesis of IPF involves the repair of lung tissue injury by alveolar epithelial cells, the differentiation and proliferation of fibroblasts, and the recruitment and activation of innate immune cells [4, 5]. Given the fact that macrophage is a typical innate immune cell, its role in the pathogenesis of pulmonary fibrosis has long been recognized [6]. Generally, macrophages manifest two distinctive phenotypes, the classically activated phenotype (M1) under the action of IFN-γ and TNF-α, and the alternatively activated phenotype (M2) under the action of IL-4, IL-13, and IL-10 [7]. Importantly, there is compelling evidence that M2 macrophages can produce copious amount of TGFβ1 to induce fibroblast differentiation and proliferation, thereby exacerbating pulmonary fibrosis [8, 9].

IL-24 is a member of the IL-20 subfamily of cytokines (IL-19, IL-20, IL-22, and IL-24), and it has two heterodimer receptor isoforms, the IL-20Rα/IL-20Rβ and IL-22R/IL-20Rβ, which are widely expressed in the skin, lungs, and reproductive tissues [10]. Current research regarding IL-24 mainly focuses on skin wound healing and tumor inhibition [11–15], while its potential role in the lung injury repair and fibrosis is yet to be tackled. It was found that IL-22 promoted extracellular matrix deposition and protease expression during the course of skin wound healing process, thereby promoting fibroblast activation and causing skin tissue remodeling [16, 17]. Importantly, IL-24 can be expressed by human and rat macrophages [18], and we further noted that IL-24 was increased both in the serum of IPF patients and the bronchoalveolar lavage fluid (BALF) of mice following bleomycin (BLM)-induced pulmonary fibrosis. Therefore, we hypothesized that IL-24 may play a critical role in the pathogenesis of fibrosis by affecting M2 program in macrophages. To address this assumption, we employed $IL-24^{-/-}$ mice to establish a lung fibrosis model via BLM induction. Our results indicated that the loss of $IL-24$ significantly attenuated BLM-induced pulmonary fibrosis and markedly reduced M2 macrophages in the lung. In agreement with the above observations, depletion of macrophages in the lung or adoptive transfer of wild type (WT) M2 macrophages into the $IL-24$-deficient lung after macrophage depletion almost completely abolished the protective effect. Mechanistic studies showed that IL-24 itself does not play a role in M2 macrophage differentiation, but it enhances the potency of IL-4 for induction of M2 macrophages by regulating signal transducer and activator of transcription 6 (STAT6) phosphorylation and peroxisome proliferator-activated receptor gamma (PPAR-γ) expression. Together, our studies suggest that IL-24 synergizes with IL-4 to promote M2 program in macrophages, thereby contributing to the development of pulmonary fibrosis.
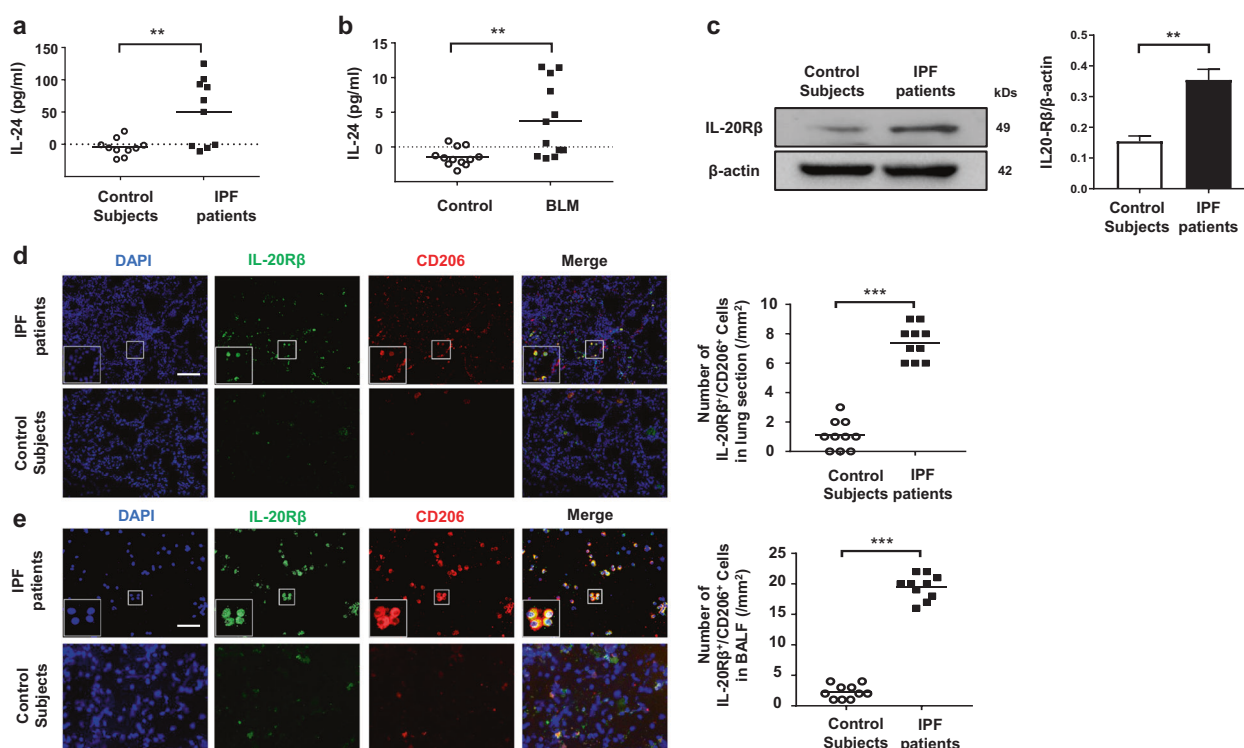
Results

Pulmonary fibrosis is featured by the increased IL-24 expression

We first sought to examine IL-24 expression in the serum of IPF patients. ELISA analysis revealed that serum IL-24 levels in control subjects were almost undetectable, while high levels of IL-24 were detected in the serum of IPF patients (Fig. 1a). Similarly, high levels of IL-24 were noted in the BALF of mice with BLM-induced pulmonary fibrosis (Fig. 1b). Given that IL-24 receptors are mainly dependent on the restrictive expression of IL-20Rβ in certain non-haemopoietic tissues including lung [10], we examined the expression of IL-20Rβ in the lung homogenates derived from IPF patients and control subjects. Western blot analysis indicated increased expression of IL-20Rβ in IPF patients (Fig. 1c). Additionally, as M2 macrophages are the main infiltrating cells in the lungs of patients with IPF, we conducted co-immunostaining of lung sections derived from IPF patients and control subjects with IL-20Rβ (IL-24 receptor) and CD206 (a marker for M2 macrophages). The number of IL-20Rβ$^+$/CD206$^+$ cells in IPF patient-derived lung sections was significantly increased as compared to that of control subjects (Fig. 1d). To confirm this result, we next checked BALF from IPF patients by co-immunostaining of IL-20Rβ and CD206, and interestingly found that M2 macrophages were the predominant cells manifesting IL-20Rβ overexpression (Fig. 1e). Next, we examined the expression of other IL-24 receptors (i.e., IL-20Rα and IL-22R) in CD206$^+$ macrophages. Interestingly, we only detected very low levels of IL-20Rα and IL-22R expression in M2 macrophages in the lung sections originated from IPF patients and control subjects (Supplementary Fig. 1). Collectively, these data suggest that pulmonary fibrosis manifests altered IL-24 expression along with overexpression of its cognate receptor IL-20Rβ during disease development.

Loss of IL-24 attenuates BLM-induced lung injury and fibrosis

Based on the above observations, we next sought to demonstrate the effect of IL-24 on pulmonary fibrosis by using $IL-24^{-/-}$ and WT mice following BLM induction. The severity of lung injury and fibrosis following 21 days of BLM induction were significantly attenuated in $IL-24$-deficient mice. Specifically, the H&E, Masson's trichrome, and Sirius red staining indicated that lung injury and pulmonary fibrosis were significantly attenuated in the $IL-24^{-/-}$ mice (Fig. 2a, left panel). In particular, the severity of pulmonary fibrosis was substantially lower as evidenced by the lower Ashcroft scores (Fig. 2a, right

Fig. 1 Analysis of IL-24 expression in IPF patients and in BLM-induced mice. a ELISA analysis of IL-24 levels in the serum from IPF patients and healthy subjects. A total of ten IPF patients and ten control subjects were analyzed. Results are shown as the median; each dot represents one patient. The dotted line indicates the detection limit. Statistical analysis was performed using the Student's t test (**$p <$ 0.01). **b** ELISA analysis of IL-24 levels in the BALF of mice following 21 days of BLM induction. Twelve mice were analyzed in each group. Each dot represents an animal, and the median is presented. The dotted line indicates the detection limit. Statistical analysis was performed using the Student's t test (**$p < 0.01$). **c** Western blot analysis of IL-20Rβ expression in the lung homogenates derived from IPF patients and control subjects. Left panel: a representative Western blot result. Right panel: a bar graph showing the mean data for five IPF patients and five control subjects analyzed. Statistical analysis was performed using the Student's t test (**$p < 0.01$). **d** Representative results for co-immunostaining of IL-20Rβ and CD206 (an M2 macrophage marker) in the lung sections from patients with IPF and healthy subjects. The nuclei were stained blue by DAPI, Scale bar, 50 μm. A total of ten IPF patients and ten control subjects were analyzed. Scatter plot indicates the IL-20Rβ$^+$/CD206$^+$ cell count (numbers/mm^2) in the lung sections from IPF patients and healthy subjects; each dot represents a patient. Statistical analysis was performed using the Student's t test (***$p < 0.001$). **e** Representative results for co-immunostaining of IL-20Rβ and CD206 (an M2 macrophage marker) in the BALF from patients with IPF and healthy subjects. The nuclei were stained blue by DAPI, Scale bar, 50 μm. A total of ten IPF patients and ten control subjects were analyzed. Scatter plot indicates the IL-20Rβ$^+$/CD206$^+$ cell count (numbers/mm^2) in the BALF from IPF patients and healthy subjects; each dot represents a patient. Statistical analysis was performed using the Student's t test (***$p < 0.001$). BLM bleomycin, IPF idiopathic pulmonary fibrosis.

panel). Consistently, Western blot analysis indicated decreased expression of the fibrogenic markers fibronectin (Fib) and collagen I (Coll I) in BLM induced *IL-24*$^{-/-}$ mice (Fig. 2b). We also determined the hydroxyproline content in the lung homogenates, a marker correlated with fibrosis severity, and found that the hydroxyproline level in BLM-induced *IL-24*$^{-/-}$ mice was much lower than that in WT mice (Fig. 2c). Interestingly, following day 7 of BLM induction, both WT and *IL-24*$^{-/-}$ mice manifested a significant weight loss, a common phenotype usually associated with pulmonary fibrosis [19–21], although a temporal increase in body weight was observed after this point. Importantly, *IL-24*$^{-/-}$ mice had significantly less weight loss at days 7 and 14 after BLM induction, and a similar trend was also observed at day 21 (Fig. 2d), which

was likely caused by the differences of the severity for lung injury and inflammatory responses. Taken together, these results indicate that loss of IL-24 protects mice against BLM-induced lung injury and fibrosis.

IL-24 deficiency represses BLM-induced TGF-β1 signaling

Given that TGF-β1 plays an important role in the progression of pulmonary fibrosis, we thus next examined TGF-β1 expression in the lung. First, we conducted RT-PCR analysis of TGF-β1 mRNA. *IL-24*$^{-/-}$ mice had significantly lower TGF-β1 mRNA expression after BLM induction (Fig. 3a). Next, we conducted ELISA analysis of matured TGF-β1 in the BALF. TGF-β1 secretion in
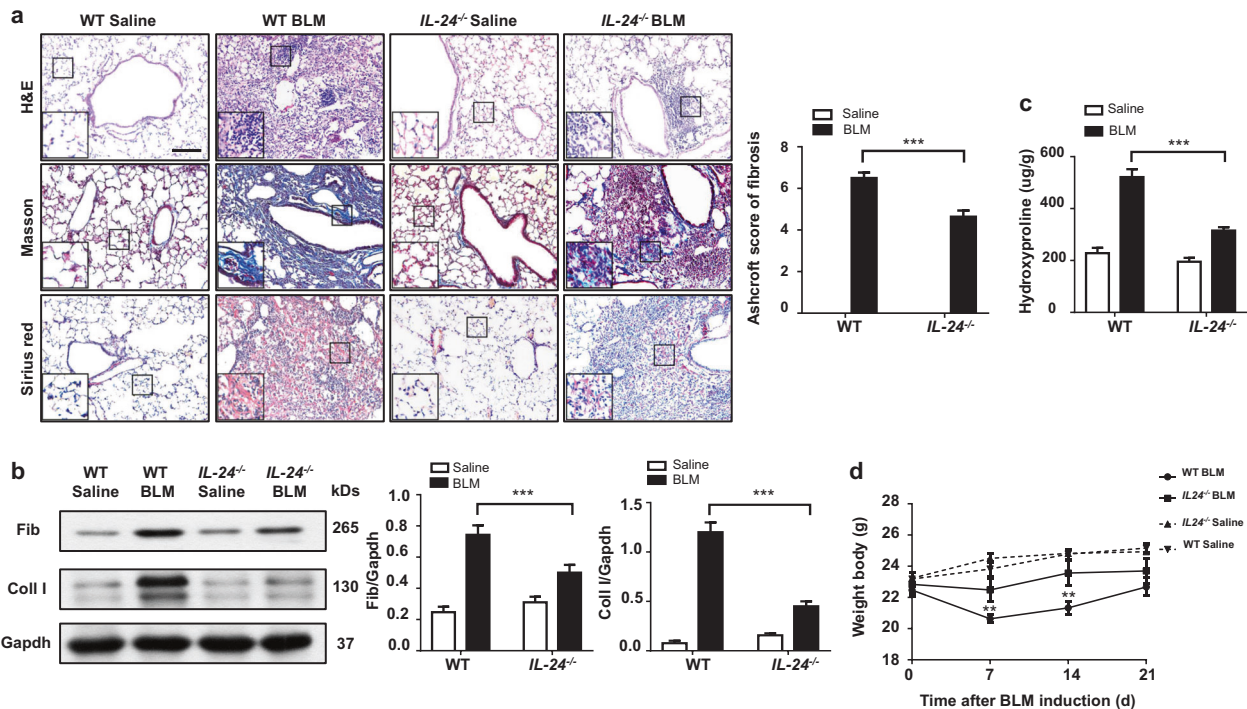
Fig. 2 Loss of IL-24 attenuates lung injury and fibrosis. a Histological analysis of the severity of lung fibrosis in mice after BLM induction. Left panel: representative results for H&E (top), Masson (center), and Sirius red (bottom) staining. The insets show higher magnification images for a particular location. Right panel: a bar graph showing the semiquantitative Ashcroft scores for the severity of fibrosis, Scale bar, 50 μm. Error bars represent means ± SEM ($n = 12$). Statistical analysis was performed using one-way ANOVA (***$p <$ 0.001). **b** Western blot analysis of the fibrotic markers collagen I and fibronectin. Left panel: a representative Western blot result. Right panel: a bar graph showing the mean data for all mice analyzed in each group. Error bars represent means ± SEM ($n = 12$). Statistical analysis was performed using one-way ANOVA (***$p < 0.001$). **c** Bar graph showing the quantification of hydroxyproline content in the lungs of mice after BLM induction. Error bars represent means ± SEM ($n = 12$). Statistical analysis was performed using one-way ANOVA (***$p < 0.001$). **d** Body weight changes during the course of BLM-induced fibrosis. Error bar represents the mean ± SEM of 12 mice analyzed. Statistical analysis was performed using one-way ANOVA (**$p < 0.01$). BLM bleomycin, Coll I collagen I, Fib fibronectin, WT wild type.

BLM-induced $IL-24^{-/-}$ mice was markedly lower than that in WT mice (Fig. 3b). In line with this observation, the downstream phosphorylated Smad2 and Smad3 levels in BLM-induced WT mice were substantially higher than that in $IL-24^{-/-}$ mice (Fig. 3c), although there was no perceptible difference in terms of total Smad2/3 between $IL-24^{-/-}$ and WT mice. Co-immunostaining of BLM challenged lung sections further revealed that M2 macrophages (CD206^{+}) were the predominant cells for secretion of TGF-β1. However, $IL-24^{-/-}$ mice exhibited markedly less TGF-β1^{+}/CD206^{+} cells following BLM induction (Fig. 3d), and similar results were also observed by flow cytometry analysis of gated F4/80 macrophages (Fig. 3e). Of note, other than macrophages, positive staining of TGF-β1 was also observed in other cell types (Fig. 3d, indicated by white arrows), and single-cell sequencing also confirmed this observation (Supplementary Fig. 4). Together, our data indicate that $IL-24$ deficiency reduces the number of M2 macrophages along with decreased TGF-β1 secretion, thereby attenuating Smad2/3 signaling following BLM induction.

The protection conferred by *IL-24* deficiency relies on reduced M2 macrophages

To further investigate whether the protective effect observed in $IL-24^{-/-}$ mice was dependent on the reduction of M2 macrophages, we first depleted macrophages by intratracheal injection of clodronate liposomes into $IL-24^{-/-}$ and WT mice, and mice injected with PBS liposomes were served as the controls (Fig. 4a). As expected, almost all macrophages were depleted, and a fivefold reduction in terms of total cell number was observed in the lung as compared with that of liposomes-treated mice following day 2 of clodronate injection (Fig. 4b). Next, WT and $IL-24^{-/-}$ mice were induced with BLM as above to induce pulmonary fibrosis 1 day after clodronate liposome administration (Fig. 4a). As expected, administration of chlodronate liposomes attenuated BLM-induced lung injury and fibrosis both in WT and $IL-24^{-/-}$ mice, but more importantly, the WT and $IL-24^{-/-}$ mice displayed comparable disease severity as manifested by the similar histological changes and Ashcroft scores (Fig. 4c). Indeed, Western blot analysis
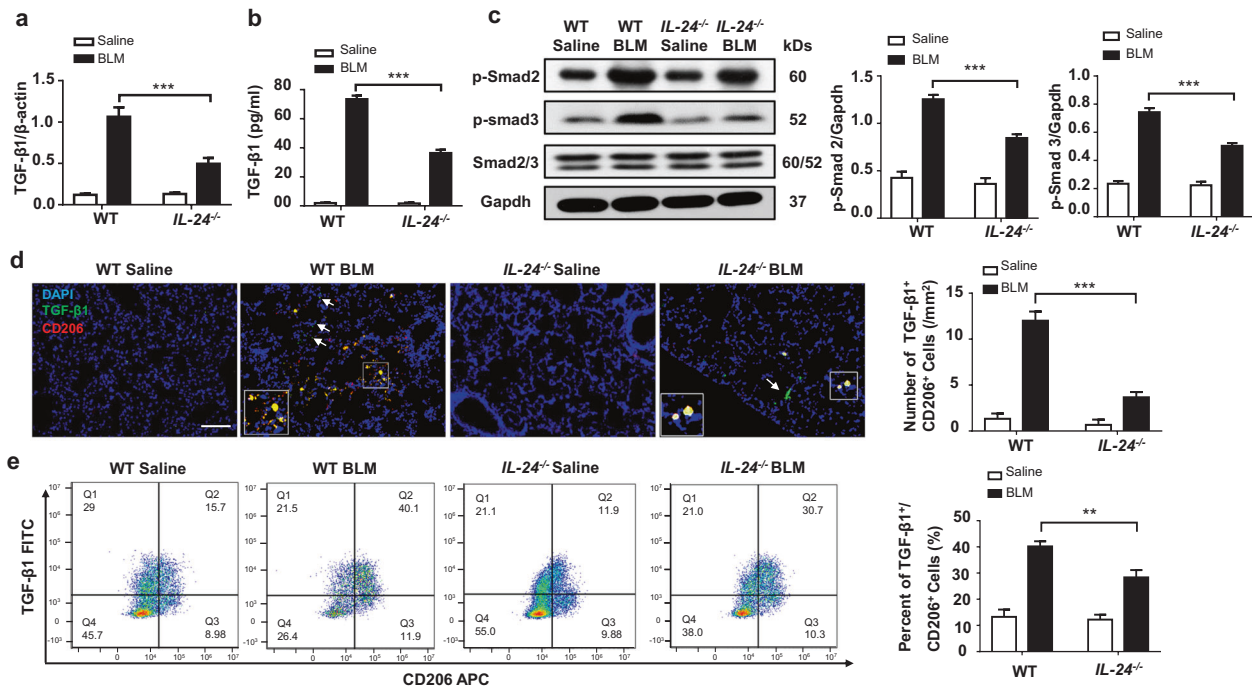
Fig. 3 Loss of IL-24 attenuates TGF-β1 signaling after BLM induction. a RT-PCR analysis of TGF-β1 expression in the lung homogenates. **b** ELISA results for TGF-β1 levels in the BALF. Error bar represents the mean ± SEM of 12 mice analyzed. Statistical analysis was performed using one-way ANOVA (***$p < 0.001$). **c** Results for Western blot analysis of TGF-β1 and downstream Smad2 and 3 activities. Left panel: a representative Western blot result for Smad2/3, p-Smad2, and p-Smad3 in the lung homogenates. Right panel: a bar graph showing the results for all mice examined. Error bar represents the mean ± SEM of 12 mice analyzed. Statistical analysis was performed using one-way ANOVA (***$p < 0.001$). **d** Co-immunostaining of TGF-β1 and CD206 in the lung sections. Scale bar, 50 μm.

The white arrows indicate TGF-β1+/CD206− cells in the lung sections. Error bar represents the mean ± SEM of 12 mice analyzed. Statistical analysis was performed using one-way ANOVA (***$p < 0.001$). **e** Flow cytometry analysis of TGF-β1 and CD206 expression in the lung single-cell suspensions in both BLM induced WT and $IL-24^{-/-}$ mice. Left panel: a scatter diagram for flow cytometry analysis. Right panel: a bar graph showing the data with five mice examined, the cells were first gated in F4/80 and CD11b, and then subjected to analysis of TGF-β1-FITC and CD206-APC expressions. Error bar represents the mean ± SEM of five mice analyzed. Statistical analysis was performed using one-way ANOVA (**$p < 0.01$). BALF bronchoalveolar lavage fluid, BLM bleomycin, TGF-β1 transforming growth factor β1.

further confirmed similar levels of fibronectin and collagen I expression in the lung between WT and $IL-24^{-/-}$ mice following BLM induction (Fig. 4d).

Next, we conducted BLM induction in $IL-24^{-/-}$ and WT mice following macrophage depletion as above, and IL-4-induced WT M2 BMDMs were then adoptively transferred into clodronate liposome-treated or PBS liposome-treated WT and $IL-24^{-/-}$ mice through intratracheal injection at day 7 of BLM induction (Fig. 5a). Similar as above, both WT and $IL-24^{-/-}$ mice with adoptively transferred BMDMs developed severe lung injury and fibrosis following BLM induction. Importantly, no significant difference in terms of disease severity was noted between WT and $IL-24^{-/-}$ mice, as evidenced by the comparable histological changes and Ashcroft scores (Fig. 5b). Consistently, WT and $IL-24^{-/-}$ mice displayed comparable fibronectin and collagen I expression levels in the lung (Fig. 5c). Collectively, these results suggest that $IL-24$ deficiency protects mice from BLM-induced lung injury and fibrosis depending on the reduction of M2 macrophages.

IL-24 synergizes with IL-4 to promote M2 program in macrophages

To dissect the mechanisms by which $IL-24$ deficiency represses M2 program in macrophages, we examined lung sections after BLM induction to characterize the cells with altered IL-24 receptor expressions. Similar to the data derived from IPF patients (Fig. 1d, e). The IL-24 receptor (IL-20Rβ) was predominantly overexpressed by the infiltrated macrophages (Fig. 6a). Furthermore, less number of IL-20Rβ+/F4/80+ cells in the lung single-cell suspension of $IL-24^{-/-}$ mice following BLM induction were also noted by flow cytometry analysis of gated F4/80 macrophages (Fig. 6b). Importantly, arginase-1, a marker for M2 macrophages, was highly expressed in F4/80+ cells, but the number of arginase-1+/F4/80+ cells was reduced in $IL-24^{-/-}$ mice as compared to that of BLM-induced WT mice (Fig. 6c), indicating that those IL-20Rβ+ macrophages manifested an M2 phenotype, and loss of $IL-24$ likely attenuated M2 program in macrophages. Flow cytometry analysis of CD11c−/CD206+ cells in the lung single-cell
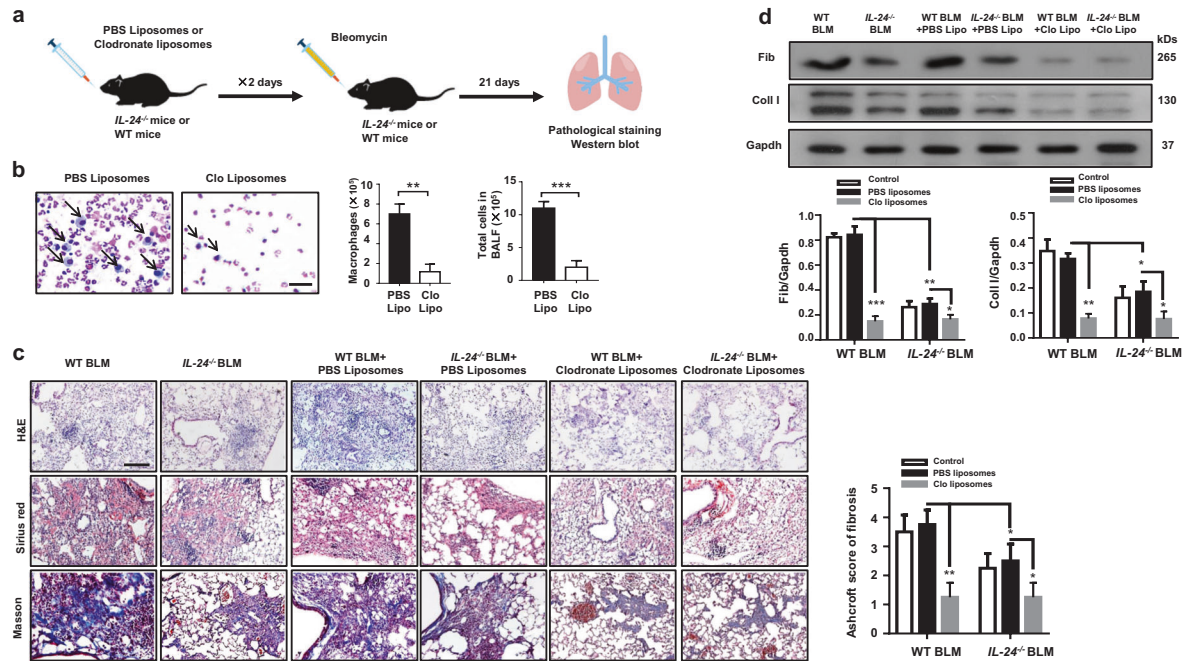
Fig. 4 Depletion of macrophages abolishes the protective effect conferred by IL-24 deficiency on BLM-induced lung injury and fibrosis. a A schematic diagram for the macrophage depletion. Macrophages were depleted by intratracheal injection of clodronate liposomes, and injection of PBS liposomes were served as the controls. **b** Clodronate liposomes efficiently depleted macrophages in the lungs; macrophages were almost undetectable in the BALF of clodronate liposomes-treated mice along with a significant reduction in total cell numbers, Scale bar, 25 μm. Error bars represent means ± SEM ($n = 5$). Statistical analysis was performed using the Student's t test (**$p < 0.01$; ***$p < 0.001$). **c** Depletion of macrophages restored $IL-24^{-/-}$ mice with manifestations similar as WT mice following BLM induction, as evidenced by the comparable histological changes and Ashcroft scores. Left panel: representative results for H&E, Sirius red, and Masson staining. Scale bar, 50 μm. Right panel: a bar graph showing the semiquantitative Ashcroft scores for the severity of fibrosis. Error bars represent means ± SEM ($n = 5$). Statistical analysis was performed using one-way ANOVA (*$p < 0.05$; **$p < 0.01$). **d** Macrophage-depleted WT and $IL-24^{-/-}$ mice manifested comparable levels of collagen I and fibronectin expression in the lung following BLM induction. Error bar represents the mean ± SEM of five mice analyzed. Statistical analysis was performed using one-way ANOVA (*$p < 0.05$; **$p < 0.01$; ***$p < 0.001$). BALF bronchoalveolar lavage fluid, BLM bleomycin, Clo Lipo clodronate liposomes, Coll I collagen I, Fib fibronectin, WT wild type.

suspension of WT and $IL-24^{-/-}$ mice following BLM induction further confirmed this observation (Fig. 6d). We thus next conducted Western blot and RT-PCR analyses of lung homogenates from BLM-induced WT and $IL-24^{-/-}$ mice for the three M2 macrophage markers, arginase-1 (Fig. 6e), *Fizz1* (Fig. 6f), and *Mgl-1* (Fig. 6g). Since *IL-24* deficiency reduced the number of M2 macrophages (Fig. 6c, d) coupled with low levels of M2 macrophage markers expression (Fig. 6e–g) in animals, our data suggest that IL-24 is probably capable of enhancing M2 program in macrophages.

To address the above notion, $IL-24^{-/-}$ mice-derived BMDMs were subjected to stimulation with IL-4, IL-24, and IL-4 plus IL-24, respectively. In contrast to our expectation, flow cytometry analysis revealed that IL-24 stimulation alone did not result in a significant difference between control BMDMs in terms of the number for F4/80$^+$/CD206$^+$ M2 macrophages. However, once IL-24 co-stimulated with IL-4, a significantly higher number of M2 macrophages were induced as compared to that of IL-4 alone stimulated cells (Fig. 7a). Similar results were observed by Western blot analysis of arginase-1 expression (Fig. 7b), and RT-PCR analysis of *Fizz1* (Fig. 7c) and *Mgl-1* expression (Fig. 7d). Taken together, our results support that IL-24 synergizes with IL-4 to promote M2 program in macrophages.

IL-24 represses SOCS1/3 activity to enhance STAT6/PPAR-γ signaling

To further determine the molecular mechanisms by which IL-24 synergizes with IL-4 to promote M2 macrophage differentiation, we studied STAT6/PPAR-γ signaling, an essential pathway for the induction of M2 macrophages [22]. To this end, $IL-24^{-/-}$ BMDMs were stimulated with either IL-4 or IL-4 plus IL-24. No significant difference was detected in terms of total STAT6 and phosphorylated STAT6 (p-STAT6) levels in BMDMs before stimulation. However, high levels of p-STAT6 were detected after 30 min of IL-4 stimulation, after which p-STAT6 underwent a steady decrease following 3 h of stimulation. A similar trend was noted for BMDMs co-stimulated with
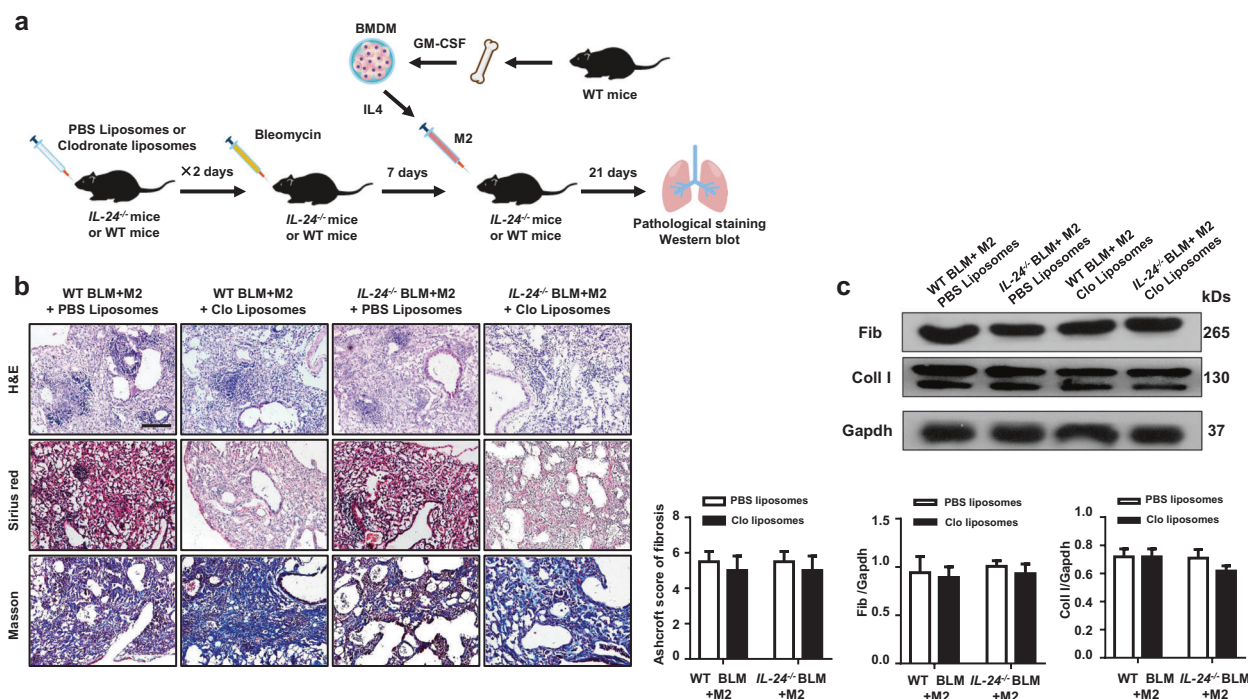
Fig. 5 IL-24 deficiency protects mice against pulmonary fibrosis relies on the reduction of M2 macrophages. a The schematic diagram for macrophage adoptive transfer studies. IL-4-induced WT M2 BMDMs were adoptively transferred into clodronate liposomes-treated or PBS liposomes-treated WT and IL-24$^{-/-}$ mice through intratracheal injection at day 7 of BLM induction. **b** Adoptive transfer of WT M2 macrophages into *IL-24*$^{-/-}$ mice restored their susceptibility to BLM-induced pulmonary fibrosis. Left panel: a representative result for H&E, Sirius red, and Masson staining, the images were taken under ×200 magnifications. Scale bar, 50 μm. Right panel displays the semiquantitative Ashcroft scores relevant to the severity of fibrosis. Error bars represent means ± SEM ($n = 5$). Statistical analysis was performed using one-way ANOVA. **c** Western blot results for analysis of collagen I and fibronectin expression in the lung homogenates from WT and *IL-24*$^{-/-}$ mice following adoptive transfer. Error bars represent means ± SEM ($n = 5$). Statistical analysis was performed using one-way ANOVA. M2 M2 macrophages, Clo clodronate liposomes, BLM bleomycin, Coll I collagen I, Fib fibronectin, WT wild type.

IL-4 and IL-24, but the p-STAT6 levels were markedly higher as compared to BMDMs stimulated with IL-4 alone at all time points examined (Fig. 8a). In consistent with these results, a steady increase in PPAR-γ expression was also observed in BMDMs following IL-4 stimulation, and the highest expression was noted following 3 h of stimulation. Importantly, BMDMs co-stimulated by IL-4 and IL-24 displayed significantly higher levels of PPAR-γ expression than that of BMDMs stimulated with IL-4 alone (Fig. 8a). However, BMDMs with IL-24 stimulation alone did not affect p-STAT6 and PPAR-γ expression at different time points (Supplementary Fig. 3a). These results prompted us to check the expression of SOCS1 and 3, inhibitors for STAT6 activity in macrophages. In general, SOCS1 is almost undetectable before stimulation, while IL-4 time-dependently induced high levels of SOCS1 and 3 expression in BMDMs, and in sharp contrast, IL-24 significantly attenuated IL-4 induced SOCS1 and 3 expression (Fig. 8b), although IL-24 alone failed to affect SOCS1 and 3 expression (Supplementary Fig. 3b). Of note, p38, ERK, JNK, Akt, and PI3K signaling are also implicated in macrophage M2 program [23–27], but it seemed that IL-24 does not have a perceptible impact on

those signaling pathways (Fig. 8c and Supplementary Fig. 3c). Altogether, our data suggest that IL-24 indirectly represses SOCS1 and 3 expression, which then enhances STAT6/PPAR-γ signaling to promote M2 program in macrophages.

Discussion

In the present report, we first demonstrated that IPF patients and mice with BLM-induced pulmonary fibrosis exhibited higher IL-24 expression than controls. Based on this observation, we then checked the function of IL-24 in pulmonary fibrosis and found that loss of *IL-24* protected mice from BLM-induced pulmonary fibrosis as characterized by the reduced TGF-β1 production and attenuated Smad2/3 signaling. Mechanistic studies showed that IL-24 alone does not have a perceptible impact on the induction of M2 macrophages, but it synergized with IL-4 to promote M2 program in macrophages. Specifically, IL-24 indirectly repressed IL-4-induced SOCS1 and 3 expression, by which it enhanced STAT6/PPAR-γ signaling to promote the M2 program together with IL-4. As a result, WT and *IL-24*$^{-/-}$
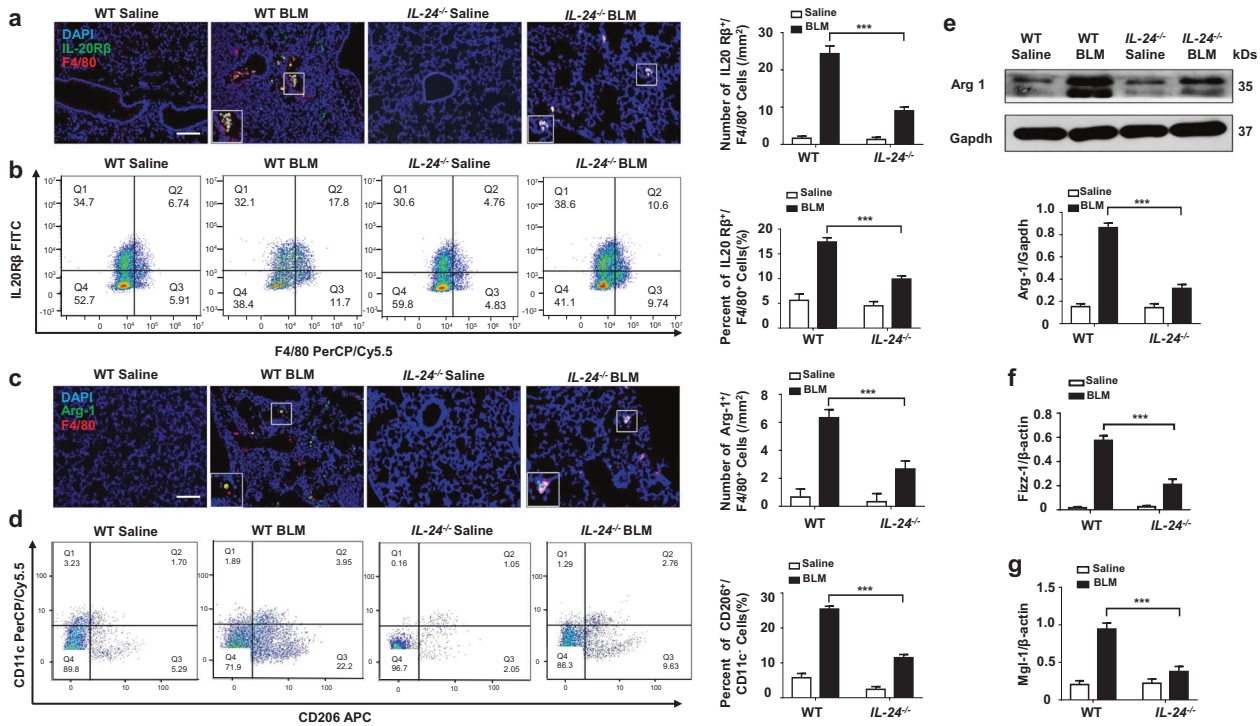
Fig. 6 IL-24 deficiency attenuates the number of M2 macrophages in the lung of mice following BLM induction. a Results for co-immunostaining of IL-20Rβ and F4/80 in BLM-induced lung sections. IL-20Rβ was significantly overexpressed in infiltrated macrophages. Scale bar, 50 μm. Error bar represents the mean ± SEM of 12 mice analyzed. Statistical analysis was performed using one-way ANOVA (***$p < 0.001$). **b** Flow cytometry analysis of IL-20Rβ and F4/80 expression in lung single-cell suspensions in both BLM induced WT and $IL-24^{-/-}$ mice. Left panel: a scatter diagram for flow cytometry analysis. Right panel: a bar graph showing the data with five mice analyzed. The L-20Rβ FITC$^+$ and F4/80-PerCP/Cy5.5$^+$ cells were gated from CD206-APC$^+$/CD11b-PE/Cy7$^+$ cells. Error bar represents the mean ± SEM of five mice analyzed. Statistical analysis was performed using one-way ANOVA (**$p < 0.01$). **c** Co-immunostaining of Arg-1 and F4/80 in the lung sections. Scale bar, 50 μm. Error bar represents the mean ± SEM of 12 mice analyzed. Statistical analysis was performed using one-way ANOVA (***$p < 0.001$). **d** Flow cytometry analysis of the number of M2 macrophage in the lung single-cell suspensions from both BLM induced WT and $IL-24^{-/-}$ mice. Left panel: a scatter diagram for flow cytometry analysis. Right panel: a bar graph showing the data with five mice analyzed. CD206-APC$^+$ and CD11c-PerCP/Cy5.5$^-$ cells were gated from the F4/80-PE and CD11b-PE/Cy7 two positive cells. Error bar represents the mean ± SEM of five mice analyzed. Statistical analysis was performed using one-way ANOVA (**$p < 0.01$). **e** Results for arginase-1 expression in the lung homogenates. Upper panel: a representative Western blot result. Lower panel: a bar graph showing the expression levels of arginase-1 in all mice examined for each group. Error bar represents the mean ± SEM of 12 mice analyzed. Statistical analysis was performed using one-way ANOVA (***$p < 0.001$). **f** Real-time PCR results for analysis of *Fizz1* expression in the lung. **g** Real-time PCR analysis of *Mgl-1* expression in the lung. Error bar represents the mean ± SEM of 12 mice analyzed. Statistical analysis was performed using one-way ANOVA (***$p < 0.001$). Arg-1 arginase-1, BLM bleomycin, Fizz1 Found in Inflammatory Zone-1, Mgl-1 Probable metabotropic glutamate receptor mgl-1.

mice displayed similar disease severity following BLM induction when WT M2 macrophages were adoptively transferred into the lungs after depletion of endogenous macrophages. Collectively, these results not only provide novel insights into the understanding of the pathoetiology underlying pulmonary fibrosis, but also demonstrate evidence suggesting that targeting IL-24 could be a viable strategy for prevention and treatment of pulmonary fibrosis in clinical settings.

There is emerging evidence that IL-20 subfamily cytokines are relevant to skin wound healing process and are associated with fibrosis. Although IL-24 is a member of the IL-20 subfamily, but most research on IL-24 has focused on its role in inflammatory skin diseases and tumorigenesis [12, 14], while no study was conducted to address its role in

fibrosis and injury repair in the lung. To address this question, we first examined IL-24 expression in the serum of IPF patients, and found that IL-24 is almost undetectable in the serum of healthy controls, which was consistent with the published data [28]. The undetectable serum IL-24 in our healthy controls was likely by that its serum levels were not high enough to be detected by this particular ELISA kit (assay range 62.5–4000 ng/ml). However, serum samples derived from IPF patients are characterized by the detection of IL-24, and consistently, high levels of IL-24 are also detected in the BALF originated from BLM-induced pulmonary fibrotic mice. We then conducted study in animals and demonstrated that mice deficient in *IL-24* were significantly protected from BLM-induced lung injury and fibrosis.
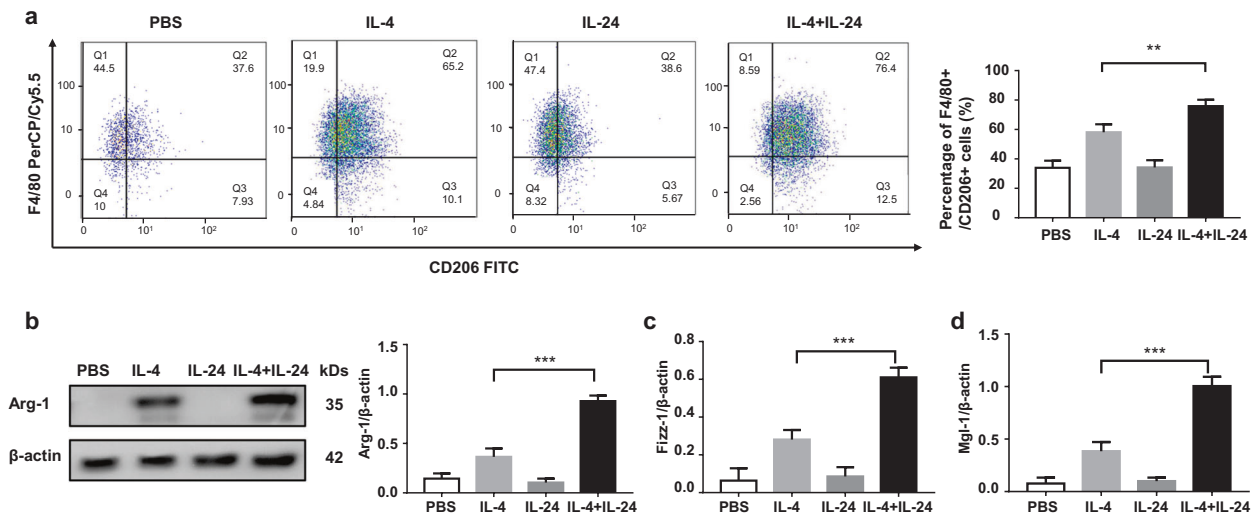
Fig. 7 IL-24 indirectly promotes the macrophage M2 program.
a Flow cytometry analysis of CD206 expression in BMDMs following stimulation with IL-4 with or without IL-24 co-stimulation. Left panel: a scatter diagram for flow cytometry analysis. Right panel: a bar graph showing the data of five mice analyzed. Error bar represents the mean ± SEM of five mice analyzed. Statistical analysis was performed using one-way ANOVA (***$p < 0.001$). **b** Results for arginase-1 expression in BMDMs following stimulation with IL-4 with in the presence or absence IL-24 co-stimulation. Error bar represents the mean ± SEM of five mice analyzed. Statistical analysis was performed using one-way ANOVA (***$p < 0.001$). Real-time PCR results for analysis of *Fizz1* (**c**) and *Mgl-1* (**d**) expression in BMDMs following stimulation with IL-4, IL-24, and IL-24/IL-4, respectively. Each bar represents the mean ± SEM of five mice analyzed. Statistical analysis was performed using one-way ANOVA (***$p < 0.001$). Arg-1 arginase-1, Fizz1 Found in Inflammatory Zone-1, Mgl-1 Probable metabotropic glutamate receptor mgl-1.

The next key question is to characterize the cells contributing to the difference in terms of disease severity between WT and $IL-24^{-/-}$ mice. We first demonstrated in the lung sections that M2 macrophages were the predominant infiltrated immune cells following BLM induction. According to previous studies [29], the enhanced macrophage M2 program is generally associated with fibrotic remodeling of internal organs, including the heart, kidneys, liver, and lungs. In particular, upon activation, M2 macrophages produce profibrotic mediators such as TGF-β1 and PDGF to induce continuous fibroblast differentiation and proliferation [30]. We thus then conducted studies and confirmed that those infiltrated M2 macrophages expressed high levels of IL-24 receptor IL-20Rβ. Next, we intend to address the impact of IL-24/IL-20Rβ axis on macrophage M2 program. Studies in $IL-24^{-/-}$ mice and BMDMs provided feasible evidence that mice deficient in $IL-24$ were significantly characterized by the blunted M2 program in macrophages.

Based on the above data, we assume that $IL-24$ deficiency may impair macrophage M2 program to protect mice from BLM-induced lung injury and fibrosis. Indeed, WT and $IL-24^{-/-}$ mice manifested comparable lung fibrosis once macrophages were depleted by clodronate liposomes, or in the condition of WT M2 macrophages were adoptively transferred into macrophage-depleted $IL-24^{-/-}$ mice. A rescue experiment was further carried out by adoptive transfer of WT M2 macrophages into $IL-24$-deficient mice without macrophage depletion. In line with our expectation, adoptive transfer of WT M2 macrophages rendered $IL-24$-deficient mice to develop a comparative disease severity as that of WT mice. Collectively, those data support that IL-24 probably modulates M2 program in macrophages to trigger the pathological processes of pulmonary fibrosis.

Given the fact that TGF-β1 serves as an essential factor for generating and maintaining a fibrotic microenvironment [31, 32], which is predominantly produced by M2 macrophages [33], we, therefore next, examined TGF-β1 expression in the lungs. As expected, BLM induced pulmonary fibrosis by enhancing macrophage infiltration along with increased TGF-β1 production. For example, BLM induced a 64-fold increase of TGF-β1 production in the BALF, whereas $IL-24$ deficiency attenuated BLM-induced TGF-β1 production by onefold. Consistently, TGF-β1 downstream signaling was significantly inhibited in $IL-24^{-/-}$ mice as featured by the decreased levels of p-Smad2 and p-Smad3, which were also essential to the pathogenesis of pulmonary fibrosis [34]. To further demonstrate how loss of $IL-24$ attenuates TGF-β1 production, we embarked on the impact of IL-24 on macrophage M2 program. Previous studies suggested that IL-4 is the most powerful inducer of M2 macrophages [7], and therefore, IL-4 was used as a positive control. Unexpectedly, IL-24 alone did not show a significant impact on M2 macrophage induction, but it
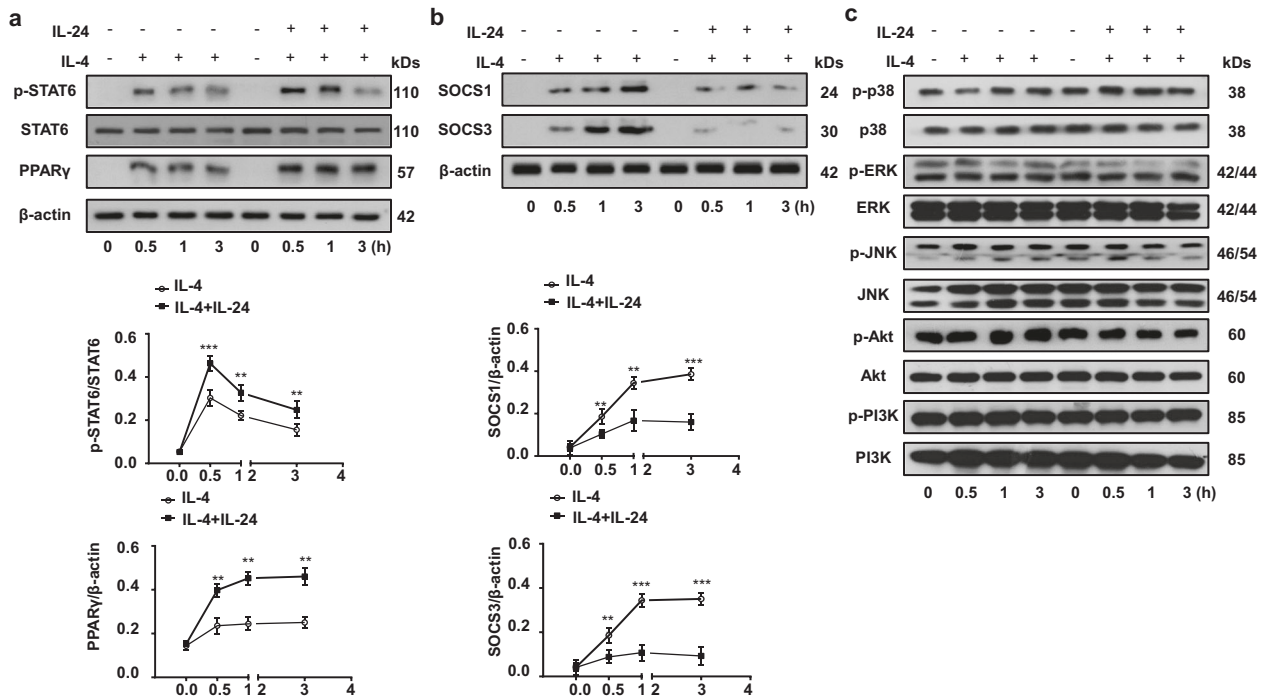
Fig. 8 The impact of IL-24 on IL-4-stimulated STAT6/PPAR-γ signaling and SOCS1/3 expression in macrophages. a IL-24 promoted IL-4-induced STAT6/PPAR-γ signaling. Upper panel: representative Western blot results for STAT6, p-STAT6, and PPAR-γ at different time points stimulated with IL-4 and IL-24/IL-4. Lower panel: figures showing the data with five mice analyzed. Statistical analysis was performed using one-way ANOVA (**$p < 0.01$; ***$p < 0.001$). **b** IL-24 indirectly repressed SOCS1/3 expression. Upper panel: representative Western blot results for SOCS1 and SOCS3 at the indicated time points following IL-4 and IL-24/IL-4 stimulation. Lower panel: figures showing the data with five mice studied. Statistical analysis was performed using one-way ANOVA (**$p < 0.01$; ***$p < 0.001$). **c** IL-24 did not affect MAPK (p38, ERK1/2, and JNK), Akt and PI3K signaling. PPAR-γ peroxisome proliferator-activated receptor gamma, p-STAT6 phosphorylated STAT6, SOCS1 and SOCS3 suppressor of cytokine signaling 1 and suppressor of cytokine signaling 3, STAT6 signal transducer and activator of transcription 6.

significantly enhanced the potency of IL-4 for induction of M2 macrophages, suggesting that IL-24 synergizes with IL-4 to promote M2 program in macrophages. It is noteworthy that other than macrophages, certain cells were also positive for TGF-β1 staining in the fibrotic lung sections (Fig. 3d, indicated by white arrows), they could be alveolar epithelial type IIcells, T cells and mesenchymal cells according to previous reports [35, 36] and our single-cell sequencing data from IPF lungs (Supplementary Fig. 4), which would be tackled in our future studies.

The last important question is how IL-24 synergizes with IL-4 to promote M2 program in macrophages. Previous studies have shown that Th2 cytokines can stimulate STAT6 phosphorylation, which then directly induces macrophage expression of M2 genes [37]. However, nuclear receptor PPAR-γ activity seems to be required for the full implementation of M2 program [38]. We therefore embarked on the impact of IL-24 on STAT6/PPAR-γ signaling. Indeed, IL-24 markedly promoted IL-4-induced STAT6 phosphorylation and PPAR-γ expression, as indicated by the significantly increased p-STAT6 and PPAR-γ levels detected in BMDMs. To further confirm these data,

we then examined the effect of IL-24 on SOCS1 and 3 expression, as they serve as negative regulators for the STAT6 signaling in macrophages [39]. Notably, macrophages stimulated with IL-4 and IL-24 had significantly lower levels of SOCS1 and SOCS3 than macrophages stimulated with IL-4 alone. Altogether, our results support that IL-24 indirectly represses SOCS1 and 3 expression in macrophages and upregulates STAT6/PPAR-γ signaling to promote IL-4-induced production of M2 macrophages.

In conclusion, we demonstrated that altered IL-24 expression is a characteristic feature during the course of pulmonary fibrosis. Therefore, mice deficient in *IL-24* are protected from BLM-induced lung injury and fibrosis. Mechanistic studies revealed that IL-24 is involved in the pathogenesis of pulmonary fibrosis by synergizing with IL-4 to promote M2 program in macrophages. Specifically, IL-24 indirectly represses SOCS1 and 3 expression to enhance STAT6/PPAR-γ signaling, thereby promoting IL-4-induced production of M2 macrophages. Together, our data suggest that targeting IL-24 could be a viable strategy for prevention and treatment of pulmonary fibrosis in clinical settings.

Table 1 Characteristics of subject.

	Serum		Lung tissue		BALF	
	IPF ($n = 10$)	Control ($n = 10$)	IPF ($n = 10$)	Control ($n = 10$)	IPF ($n = 10$)	Control ($n = 10$)
Age	58.43 ± 2.432	60.32 ± 3.483	48.23 ± 2.512	50.28 ± 2.942	56.25 ± 1.453	61.25 ± 2.542
Sex						
Male	6 (60%)	5 (50%)	3 (30%)	5 (50%)	6 (60%)	5 (50%)
Female	4 (40%)	5 (50%)	7 (70%)	5 (50%)	4 (40%)	5 (50%)
FVC, %	56.03 ± 4.254	NA	57.16 ± 3.657	NA	46.43 ± 3.537	NA
DLCO, %	43.74 ± 3.232	NA	41.13 ± 3.475	NA	39.48 ± 4.743	NA

IPF idiopathic pulmonary fibrosis, *BALF* bronchoalveolar lavage fluid, *DLCO* diffusion capacity for carbon monoxide, *FVC* forced vital capacity.

Materials and methods

Human samples

Serum, lung tissue, and BLAF from patients with IPF and healthy donors were collected in the Affiliated Hospital of Guilin Medical University and Tongji Hospital. IPF was diagnosed according to the ATS/ERS consensus diagnostic criteria [40]. The study was approved by the Human Assurance Committee of the Affiliated Hospital of Guilin Medical University and the Human Assurance Committee of Tongji Hospital. Clinical data and pulmonary function test results are provided in Table 1. Informed consent was obtained from all participants.

Animals

IL-24 knockout (IL-$24^{-/-}$) mice were generated as previously reported [41] and the expression of IL-24 was confirmed by Western blot (Supplementary Fig. 2). WT (C57BL/6) mice were purchased from the Animal Experimental Center of Hubei province (Wuhan, China). All animals were housed in a specific pathogen-free animal facility at the Tongji Medical College under a 12:12 h light/dark photocycle and were provided with food and water ad libitum. All experimental procedures were approved by the Animal Care and Use Committee at the Tongji Hospital. Both male and female mice were used in all experiments.

Reagents and antibodies

Murine recombinant IL-24 was obtained from R&D Systems (Minneapolis, MN, USA, # NP_444325). Murine recombinant IL-4 was obtained from Biolegend (574304), and clodronate liposomes was obtained from FormuMax (CAS: 22560-50-5). Antibodies against fibronectin, IL-20Rβ, and arginase-1 were purchased from Abcam (ab6328, ab 95824, ab60176), while antibodies against p38, p-p38, JNK, P-JNK, p-Smad2, p-Smad3, Stat6, p-Stat6, Akt, and p-Akt were obtained from Cell Signaling (9212S, 9211s,

9252S, 9255s, 3108S, 9520S, 657902, 56554s, 9272s, and 4060s). CD206, TGF-β1, Gapdh, β-actin, SOCS1, and SOCS3 antibodies were originated from Santa Cruz Biotechnology (sc-58986, Sc-146, Sc-47724, Sc-47778, Sc-9021, and Sc-9023). IL-24, ERK1/2, and p-ERK1/2 antibodies were purchased from R&D Systems (MAB2786, AF1576, and AF1018). Anti-mouse F4/80-PE, F4/80-PerCP/Cy5.5, CD11b-PE/Cy7, CD11c-PerCP/Cy5.5, CD11c-APC, CD206-FITC, and CD206-APC were purchased from Biolegend (123110, 123128, 101216, 117328, 301614, 141710, and 141708).

BLM induction of pulmonary fibrosis

WT and IL-$24^{-/-}$ mice (8–10 weeks old) were randomized to BLM-induced pulmonary fibrotic mice group or saline group. The BLM-induced pulmonary fibrotic mice group was anesthetized with 1% pentobarbital sodium and were then administered 2 U/kg BLM (Nippon Kayaku, Japan, H20090885) in 30 μl of normal saline via the intratracheal route as reported [42]. Mice administered with same volume of normal saline served as controls, and the mice were sacrificed 21 days after BLM administration for analysis of pulmonary fibrosis. Sample sizes were determined according to G Power calculations and approved by the Institutional Ethics Committee, and randomly assigned to treatment groups, non-blinded due to the nature of disease progression.

Preparation of BALF

BALF was collected by cannulating the trachea and lavaging the lung with 0.6 ml of sterile PBS using the established techniques [43]. Approximately 0.4 ml of BALF was routinely recovered from each animal.

Histological and immunohistochemical analysis

The left lung was inflated with 4% neutral buffered paraformaldehyde by 25 cm of H_2O pressure for 1 min, and the lungs were removed and placed in fresh 4% neutral

buffered paraformaldehyde for 24 h at room temperature, followed by paraffin embedding and histological analysis as previously reported. Each successive field was individually assessed for the severity of interstitial fibrosis in a blinded fashion by two pathologists using the Ashcroft scoring system [44], and six mice were included in each group. For immunostaining, the lung section was probed with first antibody (CD206, F4/80, TGF-β1, IL-20Rβ, or Arg-1) and then stained with the fluorescent secondary antibody of corresponding species (Invitrogen, San Diego, CA).

ELISA

The IL-24 level in the serum were measured using an IL-24 ELISA kit for human (RD DY1965), and the IL-24 level in the BALF were measured using an IL-24 ELISA kit for mice (RD DY2786-05). The TGF-β1 levels in the BALF were measured with a TGF-β1 ELISA kit (eBioscience, San Diego, CA) using the established techniques [45].

Culture and treatment of primary BMDMs

Primary BMDMs were obtained from male mice as previously reported [46]. Bone marrow cells first underwent lysis of red blood cells and were then resuspended in 50 ml of RPMI 1640 culture medium containing 10% fetal bovine serum, penicillin/streptomycin, and 30 ng/ml macrophage colony-stimulating factor. The cells were next plated in 35×15-mm tissue culture dishes and maintained at 37 °C, and the culture medium was changed every 2 days. After 7 days, the differentiated macrophages were cocultured with IL-4 (10 ng/ml), IL-24 (10 ng/ml) or both for the indicated time.

Macrophage depletion and macrophage adoptive transfer studies

Clodronate liposomes (40 μl) and PBS liposomes were administered intratracheally for two successive days 1 day before BLM induction, and the severity of pulmonary fibrosis was assessed 21 days after BLM induction. Total cell and macrophage count in the BALF were conducted using Wright–Giemsa stained cytospins to confirm the depletion of macrophages after 4 days of clodronate liposomes treatment. For adoptive transfer studies, BMDMs derived from WT mice were stimulated with IL-4 (10 ng/ml) for 12 h and were then transferred by intratracheal injection into the lungs of clodronate liposomes- or PBS liposomes-treated WT and IL-$24^{-/-}$ mice at a density of 1×10^6 cells/mouse (50 μl) at day 7 of BLM induction. The mice were sacrificed for analysis of pulmonary fibrosis 2 weeks after adoptive transfer.

Western blot analysis

Lung tissues and cultured cells were homogenized in RIPA lysis buffer (Biyuntian, China). The proteins were then subjected to Western blotting with the indicated primary antibodies using the established techniques [47].

Quantitative RT-PCR analysis

Quantitative RT-PCR analysis was performed using SYBR Premix Ex Taq (Takara Dalian, China) as previously reported [48]. The relative expression of each target gene was normalized to β-actin expression. The following primers were used for each target gene: *TGF-β1*, 5′-AAC CAA GGA GAC GGA ATA-3′ and 5′-GTG GAG TAC ATT ATC TTT GCT-3′; *Mgl-1*, 5-CAG GAT CCA GAC AGA TAC GGA-3′ and 5′-GGA AGC CAA GAC TTC ACA CTG-3′; *Fizz1*, 5′-TCC CAG TGA ATA CTG ATG AGA-3′ and 5′-CCA CTC TGG ATC TCC CAA GA-3′; *β-actin*, 5′-TGA CGT TGA CAT CCG TAA AGA CC-3′ and 5′-CTC AGG AGG AGC AAT GAT CTT GA-3′.

Flow cytometry

The cultured BMDMs were stimulated with IL-4 (10 ng/ml), IL-24 (10 ng/ml), or both for 12 h, and mononuclear cells in the lung tissue samples were obtained as previously reported [45], followed by staining with anti-mouse F4/80-PerCP/Cy5.5 along with CD206-FITC for BMDMs, or anti-mouse F4/80-PerCP/Cy5.5 or F4/80-PE, along with CD11b-PE/Cy7, CD206-APC, CD11c-PerCP/Cy5.5, TGFβ1-FITC, and IL-20Rβ-FITC for mononuclear cells, respectively. After washes, the cells were analyzed by flow cytometry. Data analysis was performed using FACS Express V3 software (De Novo Software, Glendale, CA).

Statistical analysis

Comparisons between groups were undertaken using the GraphPad Prism (version 7.0) software (GraphPad Software Inc., San Diego, CA, USA). Two experimental groups were compared using a Student's t test for paired data or a Student's t test with Welch's correction for unpaired data. For comparisons more than two groups, a one-way ANOVA with Bonferroni's correction was used. The data are presented as the mean ± SEM. In all cases, $p < 0.05$ was considered significant. $*p < 0.05$; $**p < 0.01$; $***p < 0.001$.

Compliance with ethical standards

Conflict of interest The authors declare that they have no conflict of interest.

Publisher's note Springer Nature remains neutral with regard to jurisdictional claims in published maps and institutional affiliations.

References

1. Hutchinson J, Fogarty A, Hubbard R, McKeever T. Global incidence and mortality of idiopathic pulmonary fibrosis: a systematic review. Eur Respir J. 2015;46:795–806.
2. Hopkins RB, Burke N, Fell C, Dion G, Kolb M. Epidemiology and survival of idiopathic pulmonary fibrosis from national data in Canada. Eur Respir J. 2016;48:187–95.
3. Ley B, Collard HR, King TE Jr. Clinical course and prediction of survival in idiopathic pulmonary fibrosis. Am J Respir Crit Care Med. 2011;183:431–40.
4. Desai O, Winkler J, Minasyan M, Herzog EL. The role of immune and inflammatory cells in idiopathic pulmonary fibrosis. Front Med (Lausanne). 2018;5:43.
5. Richeldi L, Collard HR, Jones MG. Idiopathic pulmonary fibrosis. Lancet. 2017;389:1941–52.
6. Wynn TA, Vannella KM. Macrophages in tissue repair, regeneration, and fibrosis. Immunity. 2016;44:450–62.
7. Pechkovsky DV, Prasse A, Kollert F, Engel KM, Dentler J, Luttmann W, et al. Alternatively activated alveolar macrophages in pulmonary fibrosis-mediator production and intracellular signal transduction. Clin Immunol. 2010;137:89–101.
8. Toossi Z, Hirsch CS, Hamilton BD, Knuth CK, Friedlander MA, Rich EA. Decreased production of TGF-beta 1 by human alveolar macrophages compared with blood monocytes. J Immunol. 1996;156:3461–8.
9. Young LR, Gulleman PM, Short CW, Tanjore H, Sherrill T, Qi A, et al. Epithelial-macrophage interactions determine pulmonary fibrosis susceptibility in Hermansky-Pudlak syndrome. JCI Insight. 2016;1:e88947.
10. Wang M, Liang P. Interleukin-24 and its receptors. Immunology. 2005;114:166–70.
11. Poindexter NJ, Walch ET, Chada S, Grimm EA. Cytokine induction of interleukin-24 in human peripheral blood mononuclear cells. J Leukoc Biol. 2005;78:745–52.
12. Menezes ME, Bhatia S, Bhoopathi P, Das SK, Emdad L, Dasgupta S, et al. MDA-7/IL-24: multifunctional cancer killing cytokine. Adv Exp Med Biol. 2014;818:127–53.
13. Poindexter NJ, Williams RR, Powis G, Jen E, Caudle AS, Chada S, et al. IL-24 is expressed during wound repair and inhibits TGFalpha-induced migration and proliferation of keratinocytes. Exp Dermatol. 2010;19:714–22.
14. Shefler I, Pasmanik-Chor M, Kidron D, Mekori YA, Hershko AY. T cell-derived microvesicles induce mast cell production of IL-24: relevance to inflammatory skin diseases. J Allergy Clin Immunol. 2014;133:e211–3.
15. Kumari S, Bonnet MC, Ulvmar MH, Wolk K, Karagianni N, Witte E, et al. Tumor necrosis factor receptor signaling in keratinocytes triggers interleukin-24-dependent psoriasis-like skin inflammation in mice. Immunity. 2013;39:899–911.

16. McGee HM, Schmidt BA, Booth CJ, Yancopoulos GD, Valenzuela DM, Murphy AJ, et al. IL-22 promotes fibroblast-mediated wound repair in the skin. J Invest Dermatol. 2013;133:1321–9.
17. Rutz S, Wang X, Ouyang W. The IL-20 subfamily of cytokines–from host defence to tissue homeostasis. Nat Rev Immunol. 2014;14:783–95.
18. Garn H, Schmidt A, Grau V, Stumpf S, Kaufmann A, Becker M, et al. IL-24 is expressed by rat and human macrophages. Immunobiology. 2002;205:321–34.
19. Cui Z, Liao J, Cheong N, Longoria C, Cao G, DeLisser HM, et al. The receptor for hyaluronan-mediated motility (CD168) promotes inflammation and fibrosis after acute lung injury. Matrix Biol. 2019;78:255–71.
20. Sun P, Li L, Zhao C, Pan M, Qian Z, Su X. Deficiency of α7 nicotinic acetylcholine receptor attenuates bleomycin-induced lung fibrosis in mice. Mol Med. 2017;23:34–49.
21. Burgy O, Wettstein G, Bellaye PS, Decologne N, Racoeur C, Goirand F, et al. Deglycosylated bleomycin has the antitumor activity of bleomycin without pulmonary toxicity. Sci Transl Med. 2016;8:326ra20.
22. Gordon S, Martinez FO. Alternative activation of macrophages: mechanism and functions. Immunity. 2010;32:593–604.
23. Lu J, Xie L, Liu C, Zhang Q, Sun S. PTEN/PI3k/AKT regulates macrophage polarization in emphysematous mice. Scand J Immunol. 2017;85:395–405.
24. Vergadi E, Ieronymaki E, Lyroni K, Vaporidi K, Tsatsanis C. Akt signaling pathway in macrophage activation and M1/M2 polarization. J Immunol. 2017;198:1006–14.
25. Hao J, Hu Y, Li Y, Zhou Q, Lv X. Involvement of JNK signaling in IL4-induced M2 macrophage polarization. Exp cell Res. 2017;357:155–62.
26. Shan M, Qin J, Jin F, Han X, Guan H, Li X, et al. Autophagy suppresses isoprenaline-induced M2 macrophage polarization via the ROS/ERK and mTOR signaling pathway. Free Radic Biol Med. 2017;110:432–43.
27. Kawano A, Ariyoshi W, Yoshioka Y, Hikiji H, Nishihara T, Okinaga T. Docosahexaenoic acid enhances M2 macrophage polarization via the p38 signaling pathway and autophagy. J Cell Biochem. 2019;120:12604–17.
28. Steinert A, Linas I, Kaya B, Ibrahim M, Schlitzer A, Hruz P, et al. The stimulation of macrophages with TLR ligands supports increased IL-19 expression in inflammatory bowel disease patients and in colitis models. J Immunol. 2017;199:2570–84.
29. Hashimoto D, Chow A, Noizat C, Teo P, Beasley MB, Leboeuf M, et al. Tissue-resident macrophages self-maintain locally throughout adult life with minimal contribution from circulating monocytes. Immunity. 2013;38:792–804.
30. Zhang L, Wang Y, Wu G, Xiong W, Gu W, Wang CY. Macrophages: friend or foe in idiopathic pulmonary fibrosis? Respir Res. 2018;19:170.
31. Noskovicova N, Heinzelmann K, Burgstaller G, Behr J, Eickelberg O. Cub domain-containing protein 1 negatively regulates TGF-beta signaling and myofibroblast differentiation. Am J Physiol Lung Cell Mol Physiol. 2018;314:695–707.
32. Yao Y, Wang Y, Zhang Z, He L, Zhu J, Zhang M, et al. Chop deficiency protects mice against bleomycin-induced pulmonary fibrosis by attenuating M2 macrophage production. Mol Ther. 2016;24:915–25.
33. Yu X, Buttgereit A, Lelios I, Utz SG, Cansever D, Becher B, et al. The cytokine TGF-beta promotes the development and homeostasis of alveolar macrophages. Immunity. 2017;47:903–12.
34. Lepparanta O, Sens C, Salmenkivi K, Kinnula VL, Keski-Oja J, Myllarniemi M, et al. Regulation of TGF-beta storage and activation in the human idiopathic pulmonary fibrosis lung. Cell Tissue Res. 2012;348:491–503.

35. Martinez FJ, Collard HR, Pardo A, Raghu G, Richeldi L, Selman M, et al. Idiopathic pulmonary fibrosis. Nat Rev Dis Prim. 2017;3:1–19.

36. Celada LJ, Kropski JA, Herazo-Maya JD, Luo W, Creecy A, Abad AT, et al. PD-1 up-regulation on CD4+ T cells promotes pulmonary fibrosis through STAT3-mediated IL-17A and TGF-β1 production. Sci Transl Med. 2018;10:eaar8356.

37. Wei Q, Sha Y, Bhattacharya A, Abdel Fattah E, Bonilla D, Jyothula SS, et al. Regulation of IL-4 receptor signaling by STUB1 in lung inflammation. Am J Respir Crit Care Med. 2014;189:16–29.

38. Odegaard JI, Ricardo-Gonzalez RR, Goforth MH, Morel CR, Subramanian V, Mukundan L, et al. Macrophage-specific PPARgamma controls alternative activation and improves insulin resistance. Nature. 2007;447:1116–20.

39. Inomata M, Into T, Nakashima M, Noguchi T, Matsushita K. IL-4 alters expression patterns of storage components of vascular endothelial cell-specific granules through STAT6- and SOCS-1-dependent mechanisms. Mol Immunol. 2009;46:2080–9.

40. Raghu G, Collard HR, Egan JJ, Martinez FJ, Behr J, Brown KK, et al. An official ATS/ERS/JRS/ALAT statement: idiopathic pulmonary fibrosis: evidence-based guidelines for diagnosis and management. Am J Respir Crit Care Med. 2011;183:788–824.

41. Wang J, Hu B, Zhao Z, Zhang H, Zhang H, Zhao Z, et al. Intracellular XBP1-IL-24 axis dismantles cytotoxic unfolded protein response in the liver. Cell Death Dis. 2020;11:17.

42. Liu P, Miao K, Zhang L, Mou Y, Xu Y, Xiong W, et al. Curdione ameliorates bleomycin-induced pulmonary fibrosis by repressing TGF-beta-induced fibroblast to myofibroblast differentiation. Respir Res. 2020;21:58.

43. Wang Q, Yu J, Hu Y, Chen X, Zhang L, Pan T, et al. Indirubin alleviates bleomycin-induced pulmonary fibrosis in mice by suppressing fibroblast to myofibroblast differentiation. Biomed Pharmacother. 2020;131:110715.

44. Miao K, Pan T, Mou Y, Zhang L, Xiong W, Xu Y, et al. Scutellarein inhibits BLM-mediated pulmonary fibrosis by affecting fibroblast differentiation, proliferation, and apoptosis. Ther Adv Chronic Dis. 2020;11:2040622320940185.

45. Wang Y, Zhu J, Zhang L, Zhang Z, He L, Mou Y, et al. Role of C/EBP homologous protein and endoplasmic reticulum stress in asthma exacerbation by regulating the IL-4/signal transducer and activator of transcription 6/transcription factor EC/IL-4 receptor alpha positive feedback loop in M2 macrophages. J Allergy Clin Immunol. 2017;140:1550–61.

46. Schwegmann A, Guler R, Cutler AJ, Arendse B, Horsnell WG, Flemming A, et al. Protein kinase C delta is essential for optimal macrophage-mediated phagosomal containment of Listeria monocytogenes. Proc Natl Acad Sci USA. 2007;104:16251–6.

47. Guo YC, Zhang M, Wang FX, Pei GC, Sun F, Zhang Y, et al. Macrophages regulate unilateral ureteral obstruction-induced renal lymphangiogenesis through C-C motif chemokine receptor 2-dependent phosphatidylinositol 3-kinase-AKT-mechanistic target of rapamycin signaling and hypoxia-inducible factor-1alpha/vascular endothelial growth factor-C expression. Am J Pathol. 2017;187:1736–49.

48. Hu Y, Yu J, Wang Q, Zhang L, Chen X, Cao Y, et al. Tartrate-resistant acid phosphatase 5/ACP5 interacts with p53 to control the expression of SMAD3 in lung adenocarcinoma. Mol Ther Oncolytics. 2020;16:272–88.